World Academy of Science, Engineering and Technology
International Journal of Mechanical and Mechatronics Engineering
Vol:10, No:7, 2016

Traction Behavior of Linear Piezo-Viscous Lubricants in Rough Elastohydrodynamic Lubrication Contacts

Punit Kumar, Niraj Kumar

***Abstract*—**The traction behavior of lubricants with the linear pressure-viscosity response in EHL line contacts is investigated numerically for smooth as well as rough surfaces. The analysis involves the simultaneous solution of Reynolds, elasticity and energy equations along with the computation of lubricant properties and surface temperatures. The temperature modified Doolittle-Tait equations are used to calculate viscosity and density as functions of fluid pressure and temperature, while Carreau model is used to describe the lubricant rheology. The surface roughness is assumed to be sinusoidal and it is present on the nearly stationary surface in near-pure sliding EHL conjunction. The linear P-V oil is found to yield much lower traction coefficients and slightly thicker EHL films as compared to the synthetic oil for a given set of dimensionless speed and load parameters. Besides, the increase in traction coefficient attributed to surface roughness is much lower for the former case. The present analysis emphasizes the importance of employing realistic pressure-viscosity response for accurate prediction of EHL traction.

***Keywords*—**EHL, linear pressure-viscosity, surface roughness, traction, water/glycol.

I. Introduction

THE mechanical components such as gears, cams, roller bearings etc. are integral parts of almost all the machines involving the transmission of motion and/or power. Such components involve highly stressed line contacts operating within the elastohydrodynamic lubrication (EHL) regime characterized with extremely thin lubricant films and significant increase in lubricant viscosity. The accurate prediction of EHL characteristics is necessary for accurate and reliable design especially for high precision aerospace and automotive applications.

Conventional EHL models are based upon the exponential pressure-viscosity response. However, there is a class of lubricants with the linear pressure-viscosity response at low pressures such as water/glycol solutions, low viscosity oils, and lubricants at high temperature. Kumar et al. [1] reported that the inlet viscosity of 2-3-dimethylpentane, octane, and toluene may be represented by a linear function of pressure within the inlet zone. The water/glycol solutions were found [2] to yield thinner films as compared to the conventional lubricants due to the linear pressure-viscosity dependence. Besides, the aircraft engine lubricants (L7808, L23699 etc.) employed in turbine bearings operating at very high temperatures are known to exhibit linear response at low pressure [1]. Furthermore, it is well known that for accurate prediction of EHL behavior, it is important to consider the effects of thermal softening, shear-thinning, and surface roughness. Several rheological models, as outlined by Kumar and Khonsari [3], have been employed in EHL studies over the last six decades. In recent years, through a series of high pressure rheological [4], [5] and EHL film thickness measurements [6]-[9], it has been demonstrated that the power-law based Carreau model describes the shear-thinning behavior pertaining to EHL lubricants quite accurately. Besides, several researchers [10]-[14] have studied the combined effect of shear-thinning and thermal softening.

As mentioned above, surface roughness is another factor that affects the EHL characteristics to a great extent. Using a deterministic description of roughness in EHL calculations, Venner and Napel [15] proved that the minimum film thickness decreases due to surface roughness, whereas the average film thickness remains nearly the same. Kweh et al. [16] presented the EHL analysis of an elliptical contact between a rough stationary surface and a smooth moving surface. Haung and Wen [17] studied the variation in pressure and oil film thickness with respect to roughness amplitude and wavelength. Hooke [18] presented a limit analysis for line contacts with transverse sinusoidal roughness operating in the elastic piezoviscous regime. Kaneta and Nishikawa [19] examined the effects of surface roughness on EHL films using the model irregularities.

The foregoing discussion reveals countless attempts to capture the realistic behavior of EHL conjunctions. However, no study is available on linear P-V lubricants under rough surface condition with or without thermal softening effect. Therefore, the present paper aims at investigating the traction behavior of such lubricants in EHL line contacts under near-pure sliding condition with due consideration to surface roughness and thermal softening effects. For the comparison with the conventional oils, the shear-thinning effect has also been taken into account by employing the power-law based Carreau model.

Punit Kumar is with the Department of Mechanical Engineering, National Institute of Technology, Kurukshetra, Haryana, India-136119 (phone: 91-8059000776, e-mail: punkum2002@yahoo.co.in).

Niraj Kumar is with the Department of Mechanical Engineering, National Institute of Technology, Kurukshetra, Haryana, India-136119 (phone: 91-1744-233447, e-mail: niraj_me01336@yahoo.com).

II. Thermal EHL Model

A. Rheological Model

The effective viscosity (η) pertaining to EHL lubricants is obtained by using the following Carreau shear-thinning model:

$$\eta = \tau / \dot{\gamma} = \mu \left[1 + \left(\frac{\mu \dot{\gamma}}{G_{cr}} \right)^2 \right]^{\frac{(n-1)}{2}} \tag{1}$$

where, μ is the low-shear viscosity. $\dot{\gamma} = \partial u / \partial y$ is the shear rate, n is the power-law index, and G_{cr} is a critical stress representing the Newtonian limit of lubricants.

B. Reynolds Equation

The dimensionless Reynolds equation for the case of EHL line contact is:

$$\frac{\partial}{\partial X}\left(\bar{\rho} H^3 \bar{F}_2 \frac{\partial P}{\partial X} \right) = K \frac{\partial}{\partial X}(\bar{\rho} H) + K \frac{S}{2} \frac{\partial}{\partial X}\left[\bar{\rho} H \left(1 - 2 \frac{\bar{F}_1}{\bar{F}_0} \right) \right] \tag{2}$$

where

$$X = \frac{x}{b}, \quad P = \frac{p}{p_H}, \quad \bar{\rho} = \frac{\rho}{\rho_o},$$

$$K = U \left(\frac{\pi}{4W} \right)^2$$

and

$$S = \frac{(u_2 - u_1)}{u_o}$$

The integral functions used in (2) are defined as:

$$\bar{F}_0 = \int_0^1 \frac{1}{\bar{\eta}} dY, \ \bar{F}_1 = \int_0^1 \frac{Y}{\bar{\eta}} dY \text{ and } \bar{F}_2 = \int_0^1 \frac{Y}{\bar{\eta}} \left(Y - \frac{\bar{F}_1}{\bar{F}_0} \right) dY \tag{3}$$

where $Y = y/h$ and $\bar{\eta} = \eta / \mu_o$

C. Boundary Conditions

$$P = 0 \text{ at } X = X_{in} \tag{4}$$

$$P = \frac{\partial P}{\partial X} = 0 \text{ at } X = X_o \tag{5}$$

D. Film Thickness Equation

$$H(X) = H_o + \frac{X^2}{2} + \frac{1}{\pi} \sum_{j=1}^{N} D_{ij} P_j + A \sin\left(2\pi X / \bar{\lambda} \right)$$

where A and $\bar{\lambda}$ are the dimensionless amplitude and wavelength of surface roughness, respectively, and D_{ij} are the influence coefficients:

$$\begin{aligned} D_{ij} = &-\left(i - j + \frac{1}{2} \right) \Delta X \left[\ln\left(\left| i - j + \frac{1}{2} \right| \Delta X \right) - 1 \right] \\ &+ \left(i - j - \frac{1}{2} \right) \Delta X \left[\ln\left(\left| i - j - \frac{1}{2} \right| \Delta X \right) - 1 \right] \end{aligned} \tag{7}$$

E. Density-Pressure-Temperature Relationship

The Tait's equation of state is used here to represent lubricant compressibility:

$$\frac{\rho_R}{\rho} = \frac{V}{V_R} = \left[1 - \frac{1}{1 + K_o'} \ln\left(1 + \frac{p}{K_o}\left(1 + K_o' \right) \right) \right] \times \left(1 + \alpha_\gamma \left(\theta - \theta_R \right) \right) \tag{8}$$

where

$$K_0 = K_{00} \exp\left(-\beta_k \theta \right).$$

F. Viscosity- Pressure-Temperature Relationship

The following Doolittle free volume equation is used here:

$$\frac{\mu}{\mu_R} = \exp\left(B \frac{V_{\infty R}}{V_R} \left[\frac{1 + \varepsilon\left(\theta - \theta_R \right)}{\frac{V}{V_R} - \frac{V_{\infty R}}{V_R}\left[1 + \varepsilon\left(\theta - \theta_R \right) \right]} - \frac{1}{1 - \frac{V_{\infty R}}{V_R}} \right] \right) \tag{9}$$

G. Load Equilibrium Equation

$$\int_{X_{in}}^{X_o} P dX = \frac{\pi}{2} \tag{10}$$

H. Mean Temperature Equation

The following mean fluid temperature equation is derived from the classical energy equation [14]:

$$\bar{\theta}_m = \frac{\left(\frac{\bar{\theta}_{S1} + \bar{\theta}_{S2}}{2} \right) - K_1 \phi \left(\psi_1 - \Gamma(1)/2 \right) + K_3 \bar{\rho} H^2 \left(\frac{\partial \bar{\theta}_m}{\partial X} \psi_2 - \frac{\lambda}{12} \frac{\partial \bar{\theta}_m}{\partial T} \right)}{\left[1 + K_2 H^2 \left(\frac{\partial P}{\partial X} \psi_2 - \frac{\lambda}{12} \frac{\partial P}{\partial T} \right) \right]} \tag{11}$$

For a detailed definition of the symbols used in the above equations, the readers may refer to Kumar and Khonsari [14].

I. Surface Temperature Equation

$$\bar{\theta}_{S1/S2} = 1 + D_{1/2} \int_{X_i}^{X} \frac{1}{H} \left(\frac{\partial \bar{\theta}}{\partial Y} \right)_{Y=0/1} \frac{dX'}{\sqrt{X - X'}} \tag{12}$$

where;

$$D_{1/2} = \frac{\pm k(\eta_o)^{1/2}\left(\frac{\pi}{8W}\right)^{3/4}}{\sqrt{\pi\rho_{1/2}c_{1/2}k_{1/2}\left[E'U\left(1\mp S/2\right)\right]R}} \quad (13)$$

III. Results and Discussion

TABLE I
INPUT PARAMETERS

Inlet density, ρ_o	864 kg/m^3
Equivalent radius of the disks, R	0.02 m
Equivalent elastic modulus, E'	2.1×10^{11} Pa
Density of gears, $\rho_{1,2}$	7850 kg/ m^3
Specific heat of lubricant, c	2000 J/kg K
Specific heat of rollers, $c_{1,2}$	460 J/kg K
Thermal conductivity of lubricant, k	0.14 W/m K
Thermal conductivity of rollers, $k_{1,2}$	47 W/m K

The thermal EHL model described in the previous section is solved using the solution algorithm presented by Kumar and Khonsari [14]. The solution domain $(-4 \le X \le 1.5)$ is discretized by using a uniform mesh with a grid size of ΔX = 0.005. The values of various input parameters used here are specified in Table I. The present analysis employs the actual rheological properties (Table II) of two lubricants, *viz*, L7808 (linear P-V oil) and PAO (conventional oil).

TABLE II
DOOLITTLE-TAIT AND CARREAU PARAMETERS [5], [20]

Parameters	Linear P-V oil (L7808)	Conventional oil (PAO)
μ_R [Pa s]	0.0029329	1.42
B	2.4473	4.422
$V_{\infty R}/V_R$	0.64289	0.6694
ε [K^{-1}]	–3.8402 × 10^{-4}	–8 × 10^{-4}
K_o'	9.8749	12.82
K_{00} [GPa]	8.4139	11.5
β_K [K^{-1}]	0.0055817	0.006
α_V [K^{-1}]	9.16 × 10^{-4}	0.0007
θ_o, θ_R [K]	493.15, 372	348, 348
α^* [GPa^{-1}]	7.1	15
n, G_{cr} [kPa]	0.3, 4000	0.74, 31

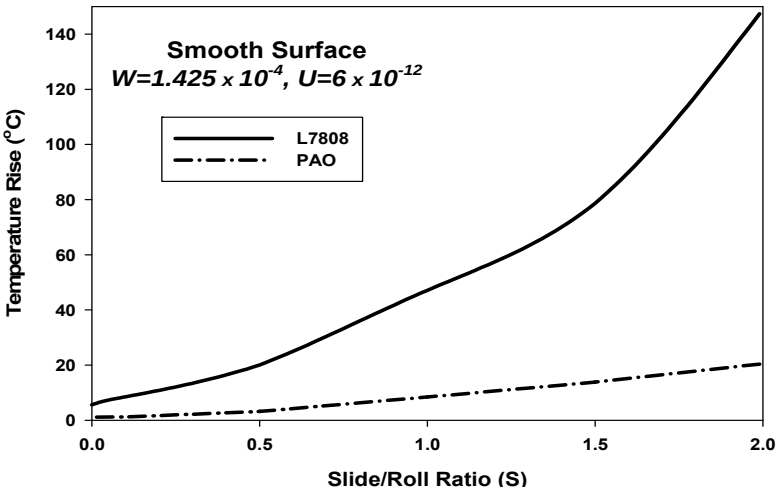

Fig. 1 Variation of temperature rise with slide/roll ratio for L7808 and PAO

A. Thermal Effect

The viscous shearing of lubricant generates substantial amount of heat leading to significant temperature rise and hence, reduction in lubricant viscosity. Therefore, Fig. 1 compares the variation of maximum temperature rise with respect to slide/roll ratio (S) for L7808 and PAO oils with the dimensionless load and speed parameters at W=1.425×10^{-4} and U=6×10^{-12} under smooth surface condition. It is quite apparent that the lubricant temperature increases with increasing slide/roll ratio; however, this increase is much more pronounced for the case of linear P-V oil (L7808) as compared to that for PAO. This is due to the fact that the inlet viscosity for the case of l7808 oil is extremely low, and hence, the rolling velocity is much higher as the value of U is equal for both the oils. Therefore, l7808 oil shears at a higher rate within the EHL conjunction leading to much more pronounced heat generation as compared to that for PAO. This is an important observation as lubricants are usually selected by comparing the minimum film thickness values predicted on the basis of dimensionless speed parameter U. However, due to the excessive heat generation, the lubricant temperature may reach its flash point in case the designer assumes isothermal conditions.

Fig. 2 compares the traction-slip characteristics pertaining to isothermal and thermal EHL analyses for the case of L7808 oil under the same operating conditions as in Fig. 1. It can be clearly seen that thermal effect causes significant reduction in the values of traction coefficient for linear P-V oils in the

same manner as for the case of conventional oils. However, as discussed subsequently, the values of traction coefficient shown in Fig. 2 are very low.

B. Speed and Load Effects

Figs. 3 (a) and (b) pertaining to L7808 and PAO, respectively, compare the variation of traction coefficient with the dimensionless speed parameter (U) for two different values of load parameter (W) indicated therein under near-pure sliding condition (S=1.99). It can be seen that the value of traction coefficient decreases with increasing speed parameter for all the cases considered here. The corresponding percentage reductions for an increase in U from 10^{-12} to 10^{-11} are indicated in Figs. 3 (a) and (b). From these values, it is evident that traction is more sensitive to the speed at higher loads, and this effect is highly pronounced for the case of PAO. Further, it can be seen that traction curves pertaining to the two values of W tend to converge with increasing speed. For L7808, the traction coefficient remains higher for higher load only up to U=2.9×10-^{12} beyond which it drops slightly. However, for the case of PAO, this "cross=over" speed parameter appears to be much beyond the range of U considered here.

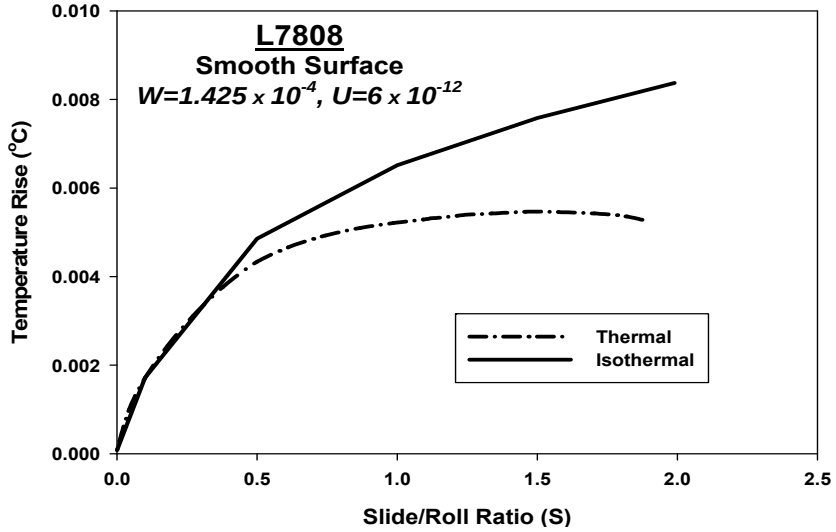

Fig. 2 Comparison of isothermal and thermal traction-slip characteristics for L7808

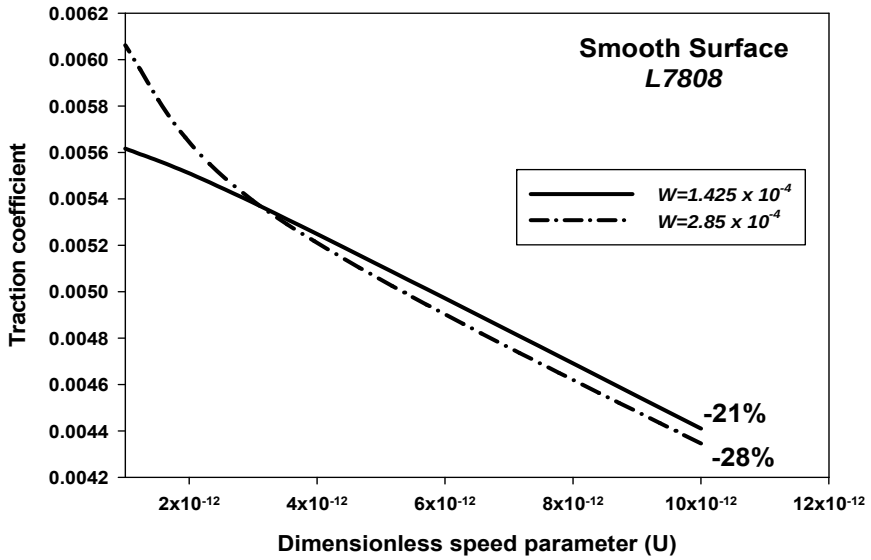

(a)

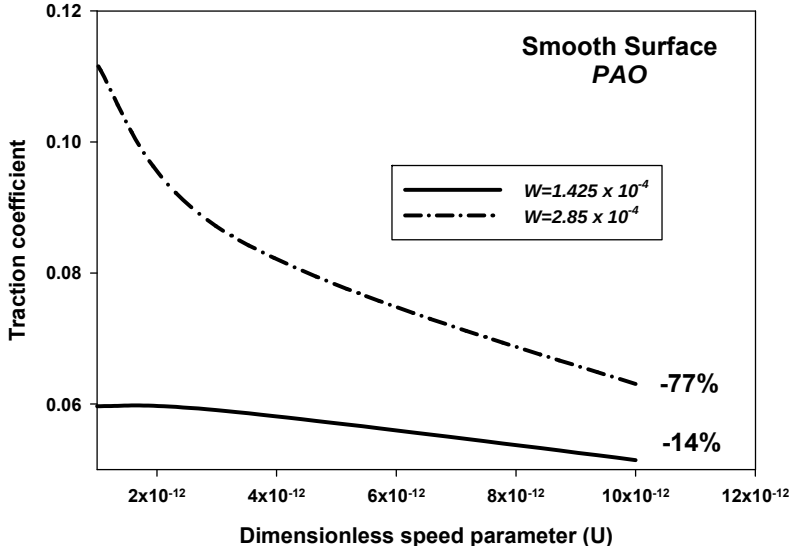

(b)

Fig. 3 Variation of traction coefficient with speed parameter at S=1.99 for (a) L7808 and (b) PAO

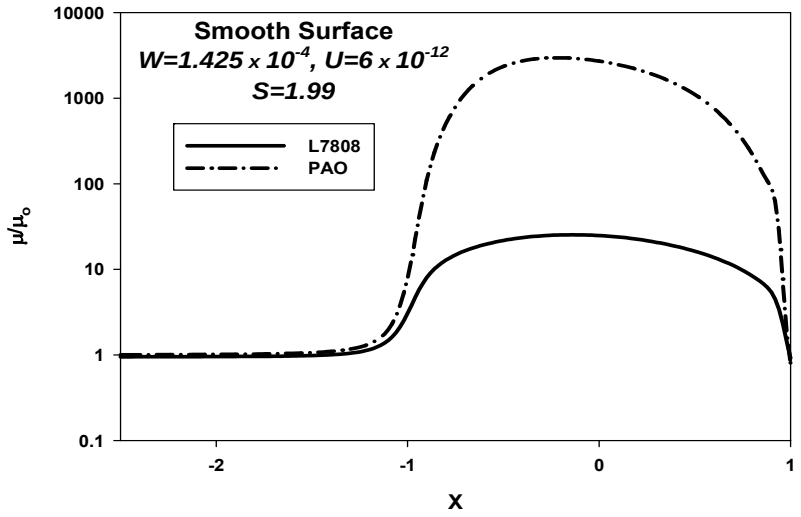

Fig. 4 Comparison of viscosity distributions for L7808 and PAO

TABLE III
COMPARISON OF FILM THICKNESS VALUES FOR TWO OILS

$W\times10^4$	$U\times10^{12}$	h_c (nm)		h_{min} (nm)	
		L 7808	PAO	L 7808	PAO
1.425	10	181	172	155	131
	3.15	96	84	84	72
	1	46	41	41	36
2.85	10	154	153	132	102
	3.15	84	74	73	52
	1	39	34	37	27

In order to explain the above observations, it is important to understand the role of various factors in this regard. The EHL traction increases with increasing contact zone viscosity and sliding velocity, while an increase in film thickness tends to reduce it. However, these factors are interdependent, for instance, film thickness depends upon viscosity which, in turn, is a function of pressure, temperature, and shear stress. The fluid temperature itself is a function of viscosity, velocity, and film thickness. Hence, the EHL traction is governed by a superposition of several interdependent effects.

While traction coefficient tends to increase with increasing speed, the associated increase in the fluid temperature leads to a reduction in viscosity. The latter effect dominates over the former under the present operating conditions and therefore, there is a net reduction in traction coefficient with increasing speed as observed in Figs. 3 (a) and (b). An increase in load causes higher pressure with a consequent increase in viscosity and hence, traction coefficient. However, this increase in viscosity tends to increase the fluid temperature as well. With increasing speed, the thermal reduction in viscosity tends to dominate over the piezo-viscous effect, which is the reason for converging curves in Figs. 3 (a) and (b). Furthermore, it may be noted that the traction coefficient values pertaining to

L7808 are over one order of magnitude lower than those for PAO even though the film thickness values for both the oils are comparable (Table III). This is attributed to extremely low contact zone viscosity for the case of L7808 as shown in Fig. 4.

C. Surface Roughness Effects

Fig. 5 compares the pressure profiles for L7808 and PAO under the rough surface condition. It can be seen that the localized pressure peaks at the asperity tips are much lower for the case of L7808. Figs. 6 (a) and (b) pertaining to L7808 and PAO, respectively, further compare the variation of traction coefficient with roughness amplitude (a) for two different values of roughness wavelength (λ) under near-pure sliding condition (S=1.99). It can be seen that the traction coefficient increases with increasing amplitude and decreasing the wavelength of surface roughness. As indicated in the figures, the percentage increase in traction coefficient for L7808 is much lower than that for PAO. In fact, it may be noted that a is increased up to 150 nm to obtain a noteworthy increase for the case of L7808, whereas it is increased only up to 100 nm for PAO.

The aforesaid increase in traction is caused by higher contact zone viscosity due to the localized pressure peaks in the presence of surface roughness. The above observations for the case of L7808 are due to lower peaks and less pronounced piezo-viscous increase in the contact zone viscosity.

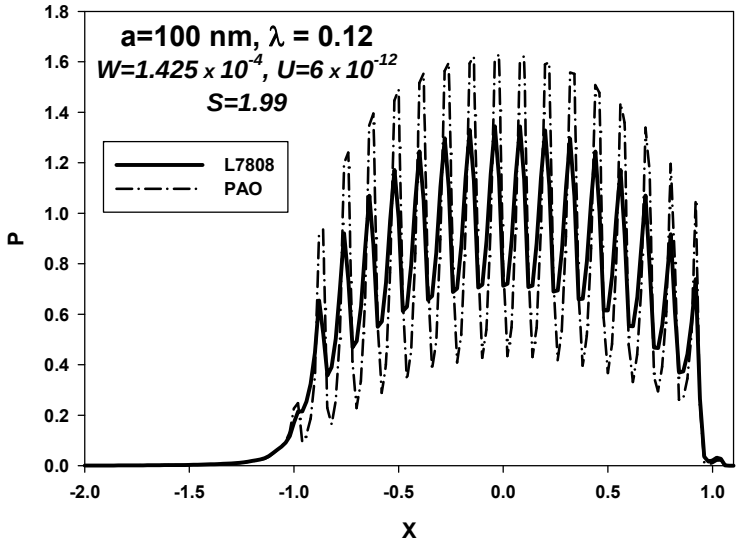

Fig. 5 Comparison of pressure profiles for L7808 and PAO

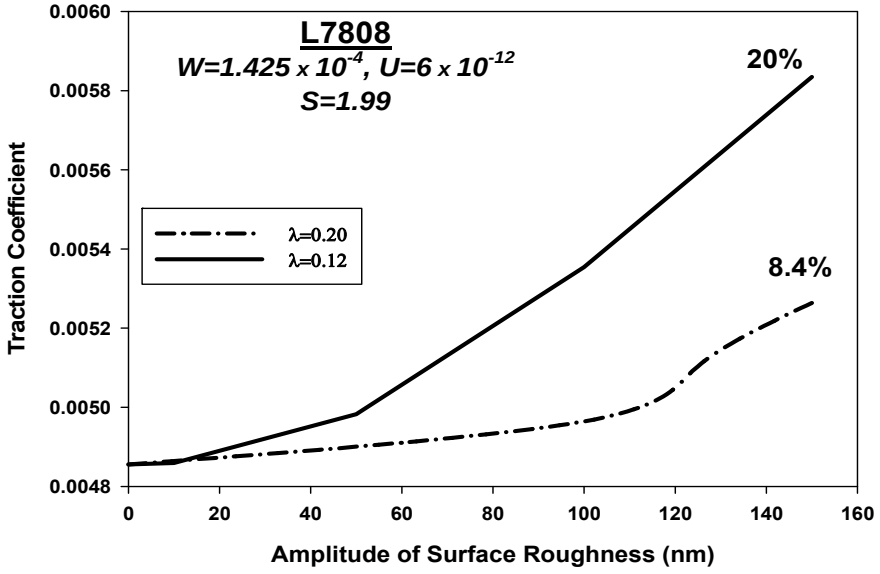

(a)

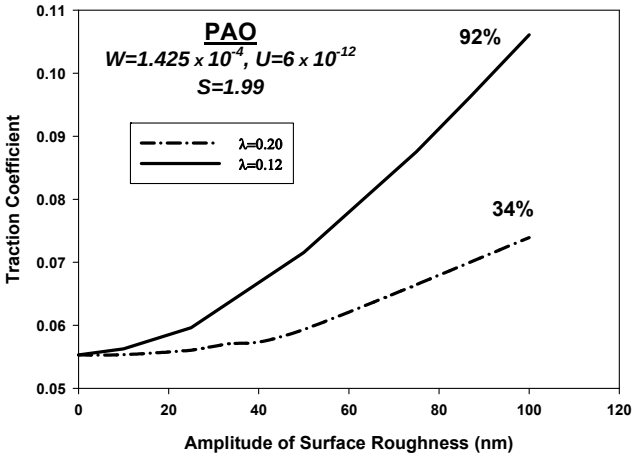

(b)

Fig. 6 Variation of traction coefficient with roughness amplitude for (a) L7808, (b) PAO

IV. Conclusions

The thermal EHL performance of lubricants with the linear pressure-viscosity (P-V) response is investigated numerically under smooth as well as rough surface conditions. The temperature modified Doolittle-Tait equations are used to determine lubricant viscosity and density as functions of pressure and temperature. The lubricant rheology is described by the power-law based Carreau shear-thinning model. In this analysis, the actual properties of two commercially used EHL lubricants, L7808 and PAO, are used to simulate the linear and conventional pressure-viscosity response, respectively. Based upon the simulation results presented in the previous section, the following conclusions are drawn:

1. The rise in lubricant temperature attributed to viscous shearing increases substantially with slide/roll ratio and this increase is found to be much more pronounced for the case of linear P-V oil (142 ^{o}C) as compared to that for conventional oil (19 ^{o}C). Therefore, it is concluded that the use of linear P-V oils should be restricted to relatively low speed parameters so that flash point temperature is not attained. Instead of minimum film thickness predictions based upon conventional formulas, a comprehensive thermal EHL analysis should form the basis of lubricant selection.
2. For a given set of dimensionless speed and load parameters, the oil with linear pressure-viscosity response is shown to yield slightly thicker EHL films along with extremely low (around one-tenth) traction coefficients as compared to the conventional oil. Also, the sensitivity of traction coefficient to speed and load is quite low for the case of linear P-V oil. Therefore, it is more suitable under conditions involving frequent variations in operating conditions.
3. The localized pressure peaks at the asperity tips for the case of linear P-V oil are found to be 20-32% lower with respect to those for conventional oil. Therefore, it is concluded that such oils significantly reduce the contact stresses under rough surface condition and hence, provide better protection against wear.
4. The traction coefficient increases with increasing amplitude and decreasing wavelength of surface roughness. For linear P-V oils, this increase in traction is not appreciable; however, for high-precision applications, it is necessary to carry out thermal EHL analyses with realistic lubricant properties and surface topography for accurate prediction of traction.

Nomenclature

b	half width of Hertzian contact zone (m)
E'	effective elastic modulus of rollers 1 and 2 (Pa).
h	film thickness (m)
H	dimensionless film thickness, $H = hR/b^2$
H_o	dimensionless offset film thickness
p	Pressure (Pa)
p_H	maximum Hertzian pressure, (Pa)
P	dimensionless pressure, $P = p/p_h$
R	equivalent radius of contact (m)
S	slide to roll ratio, $S = (u_2 - u_1)/u_o$
u_o	average rolling speed, $u_o = (u_1 + u_2)/2$, (m/s)
u_1, u_2	velocities of lower and upper surfaces, (m/s)
U	dimensionless speed parameter, $U = \frac{\mu_o u_o}{E'R}$
w	applied load per unit length (N/m)
W	dimensionless load parameter, for line contact
$\dot{\gamma}$	shear strain rate across the fluid film, (s^{-1})
ρ_o	inlet density of the lubricant (kg/m^3)
ρ	lubricant density at the local pressure (kg/m^3)
μ_o	inlet viscosity of the Newtonian fluid (Pa.s)
η	generalized Newtonian viscosity (Pa.s)

θ_o inlet temperature (K)

θ_m mean temperature (K)

REFERENCES

[1] Kumar, P., Bair, S., Krupka, I., and Hartl, M., 2010, "Newtonian Quantitative Elastohydrodynamic Film Thickness with Linear Piezoviscosity," Tribol. Int., vol.43, pp. 2159-2165.

[2] Spikes, H. A., 1987, "Wear and fatigue problems in connection with water-based hydraulic fluids," J Synthetic Lubrication, vol. 4, pp. 115-135

[3] Kumar, P., and Khonsari, M. M., 2009, "On the Role of Lubricant Rheology and Piezo-viscous Properties in Line and Point Contact EHL," Tribol. Int., vol. 42, pp. 1522-1530.

[4] Bair, S., and Qureshi, F., 2003, "The Generalized Newtonian Fluid Model and Elastohydrodynamic Film Thickness," ASME J. Tribol., vol. 125, pp. 70–75.

[5] Bair S., 2007, *High Pressure Rheology for Quantitative Elastohydrodynamics* Tribology and Interface Engineering Series 54, Elsevier Press, Amsterdam, Netherlands.

[6] Chapkov, A. D., Bair, S., Cann, P., and Lubrecht, A. A., 2007, "Film Thickness in Point Contacts under Generalized Newtonian EHL Conditions: Numerical and Experimental Analysis," Tribol. Int., vol. 40, pp. 1474-1478.

[7] Jang, J. Y., Khonsari, M. M., and Bair, S., 2007, "On the elastohydrodynamic analysis of shear-thinning fluids," Proc. Roy. Soc. London, vol. 463, pp. 3271-3290.

[8] Liu, Y., Wnag, Q. J., and Bair, S., 2007, "Vergne P, A Quantitative Solution for the Full Shear-Thinning EHL Point Contact Problem Including Traction," Tribol. Letters, vol. 28, pp. 171-181.

[9] Krupka, I., Kumar, P., Bair, S., Khonsari, M. M., and Hartl M, 2010, "The Effect of Load (Pressure) For Quantitative EHL Film Thickness," Tribol. Letters, vol. 37, pp. 613-622.

[10] Sui, P. C., and Sadeghi, F., 1991, "Non-Newtonian Thermal Elastohydrodynamic Lubrication," ASME J. Tribol., vol. 113, pp. 390-397.

[11] Salehizadeh, H., and Saka, N., 1991, "Thermal Non-Newtonian Elastohydrodynamic Lubrication of Rolling Line Contacts," ASME J. Tribol., vol. 113, pp. 181-191.

[12] Wang, S., Conry, T. F., and Cusano, C., 1992, "Thermal Non-Newtonian Elastohydrodynamic Lubrication of Line Contacts Under Simple Sliding Conditions," ASME J. Tribol., vol. 114, pp. 317-327.

[13] Hsiao, H. S., and Hamrock, B. J., 1992, "A Complete Solution for Thermal Elastohydrodynamic Lubrication of Line Contacts Using Circular Non-Newtonian Fluid Model" ASME J. Tribol., vol. 114, pp. 540-552.

[14] Kumar, P., and Khonsari, M. M., 2008, "Combined Effects of Shear Thinning and Viscous Heating on EHL Characteristics of Rolling/Sliding Line Contact," ASME J. Tribol., vol. 130, pp. 041505-1-13.

[15] Venner, C. H. and Napel, W. E. T., 1992, "Surface roughness effects in an EHL line contact," ASME J. Tribol., vol. 114, pp. 616–22

[16] Kweh, C. C., Patching, M. J., Evans, H. P., Snidle, R. W., 1992, "Simulation of elastohydrodynamic contacts between rough surfaces," ASME J. Tribol.. vol. 114, pp. 412-419,

[17] Huang, P. and Wen, S., 1992, "Study on oil film thickness and pressure distribution of micro-EHL," ASME J. Tribol., vol. 114, pp. 42-46.

[18] Hooke, C. J., 1998, "Surface roughness modification in elastohydrodynamic line contacts operating in the elastic piezoviscous regime," Proc. IMechE J. Eng. Tribol., vol. 212, pp. 145-157.

[19] Kaneta, M., Nishikawa, H., 1999, "Experimental study on microelastohydrodynamic lubrication," Proc. IMechE J. Eng. Tribol., vol. 213, pp. 371-381.

[20] Kumar, P., and Kalita, T. J., 2015, "Transient EHL Film Thickness During Normal Approach Considering Shear-thinning and Linear Piezo-viscous Oils," ASME J. Tribol., vol. 137, pp. 021504/1-7.